Diagnostic accuracy of contrast enhanced spectral mammography in assessment of indeterminate breast lesions in patients after breast conservation surgery

D.A. Mohamed Shaban*, A.A. Ghaffar Boraei, N.A.E. Tawfik Chalabi, M.A.M. Ali Nagi

Department of Radiodiagnosis, Faculty of Medicine, Ain Shams University, Cairo, Egypt

ABSTRACT

▶ Original article

*Corresponding author: Dalia A. Mohamed Shaban, M.D., E-mail:

daliaashaban@gmail.com

Received: August 2024 Final revised: May 2025 Accepted: May 2025

Int. J. Radiat. Res., October 2025; 23(4): 865-871

DOI: 10.61186/ijrr.23.4.5

Keywords: Comprehensive Diagnostic accuracy, breast cancer, contrastenhanced spectral mammography, breast lesions, breast-conserving surgeries.

Background: Breast cancer stands out as a major health issue globally, being the most common type of cancer diagnosed in women around the world. Its impact in Egypt is particularly pronounced, accounting for a substantial proportion of new cancer cases. Contrast-Enhanced Spectral Mammography (CESM) has emerged as a promising diagnostic tool for breast tumors. By visualizing tumor angiogenesis, CESM offers improved accuracy compared to traditional mammography with or without ultrasound. Its ability to depict tumor neovascularity parallels that of breast magnetic resonance imaging (MRI). This study was done to assess how well CESM can accurately identify the nature of unclear breast lesions in patients who have had breastconserving surgery (BCS). Materials and Methods: We carried out a retrospective study with 30 women who had breast-conserving surgery due to ambiguous breast lesions found by traditional mammography. Their ages varied between 32 and 77, averaging 50.07 years. Each patient received dual-energy contrast-enhanced spectral mammography. The definitive diagnosis was confirmed by examining tissue samples from surgery or biopsy through histopathology. Results: Examination of the 30 patients showed that 23 had benign lesions (69.7%) while 10 were malignant (30.3%). The diagnostic performance character of CESM was improved with the use of the malignancy potential score (MPS) in distinguishing between benign and malignant breast lesions. Conclusion: The results indicate that CESM serves as an effective supplement to traditional mammography for evaluating unclear breast lesions after breast-conserving surgery. Its enhanced sensitivity and accuracy could lead to better patient management and improved health outcomes.

INTRODUCTION

Breast cancer (BC) remains a major global health concern, representing the second leading cause of cancer-related deaths among women worldwide. In 2022, there were 2.3 million new diagnoses globally, and tragically, an approximate number of 670,000 women died from the disease. Statistics from the American Cancer Society in 2024 estimate approximately 310,720 new cases of invasive breast cancer, 56,500 new cases of ductal carcinoma in situ (DCIS), and around 42,250 deaths due to BC ⁽¹⁾.

Egypt is not exempt from breast cancer's worldwide burden, despite having a lower incidence rate compared to developed nations. However, the mortality rate in Egypt is disproportionately high, resulting in a mortality-to-incidence ratio approximately double that of developed countries. This enormous disparity highlights the critical need for effective early detection measures (2).

Breast cancer mortality rates have demonstrated a consistent descending trend since 1989, resulting in a 42% overall reduction by 2021. This notable

decrease is largely attributed to a combination of factors, including earlier detection through screening initiatives, increased public awareness of the disease, and advancements in therapeutic interventions. It is important to note, however, that the pace of this decline has been changed in recent years (3).

Early diagnosis and appropriate treatment are crucial for improving breast cancer outcomes. Consequently, developing accurate and cost-effective diagnostic tools is imperative to address the diverse needs of women across different populations and socioeconomic backgrounds (4).

Digital mammography (DMG) has become a cornerstone of breast cancer screening. However, its effectiveness is limited, especially in females with dense breast tissue. The overlapping densities of breast tissue often obscure underlying malignant masses, leading to increased false-positive (FP) results and decreased sensitivity (5).

Breast-conserving surgery (BCS) is typically the first choice for treating early-stage BC. Yet, about 20% of patients end up needing a mastectomy because of conditions like multifocal or multicentric

cancer, widespread DCIS, large tumors, or recurrent cancer (6).

Contrast-enhanced spectral mammography (CESM) is a relatively new imaging modality that combines conventional DMG with intravenous contrast administration. By exploiting the principle of tumor angiogenesis, CESM effectively highlights areas of abnormal blood vessel growth within breast tissue. This technique offers superior diagnostic accuracy compared to traditional mammography (7).

CESM shares similarities with magnetic resonance imaging (MRI) in terms of contrast enhancement patterns, suggesting comparable diagnostic applications. However, CESM surpasses MRI in several key aspects. It can readily detect microcalcifications and is free from limitations associated with ferromagnetic characteristics and design of the machine. Additionally, CESM is significantly more cost-effective and time-efficient than MRI, with shorter examination times and lower costs for equipment and contrast agents ⁽⁸⁾.

CESM generates low-energy two-dimensional mammographic images, similar to standard digital mammography. However, post-contrast image analysis enables the assessment of tumor neovascularity, a characteristic typically evaluated using magnetic resonance imaging (MRI) ⁽⁹⁾.

Breast conservation therapy (lumpectomy or segmental mastectomy followed by radiation) can result in a variety of breast alterations, including masses, fluid collections, architectural distortion, scarring, swelling (edema), skin thickening, and calcification. These changes can resemble or obscure local breast cancer signs of recurrence between benign Distinguishing post-treatment alterations and recurrent cancer can be challenging due to overlapping mammographic features (10).

Following BCS, it's important to differentiate between expected post-treatment changes and potential signs of recurrence. Post-surgical masses and fluid collections typically resolve within a year. Radiation-induced edema generally subsides over time, but increasing edema should raise concern for recurrence. The presence of interspersed radiolucent areas within a poorly defined soft tissue mass often suggests post-surgical scarring, whereas recurrent cancer typically presents as a solid mass without these radiolucencies. Finally, while pleomorphic and granular microcalcifications can be a sign of recurrence, they should be carefully distinguished from benign calcifications associated with scarring (10).

Indeterminate breast lesions, exhibiting characteristics of both benign and malignant lesions, pose a diagnostic dilemma. In high-risk women, these indeterminate findings warrant aggressive evaluation due to the heightened risk of malignancy (10).

The study hypothesized that CESM's might enhance breast lesion detection while reducing false

positive and negative results. Thus, the study aimed to evaluate the potential of CESM in improving diagnostic accuracy for postoperative breast cancer surveillance by comparing the findings from CESM with routine full-field digital mammography (FFDM) in patients who underwent breast-conserving surgery (BCS).

MATERIALS AND METHODS

This retrospective study tried to evaluate the role of CESM in assessing indeterminate breast lesions following BCS. The study was conducted at Ain Shams University hospitals and private centers between June 2019 and July 2023. Files of female patients who underwent BCS and presented with indeterminate breast lesions on Sono-mammography were eligible for inclusion without age restrictions. Exclusion criteria included the presence of severe allergy to contrast material or significant renal impairment, defined as a serum creatinine level higher than 1.8 mg/dL or an estimated glomerular filtration rate (eGFR) less than 30 mL/min/1.73 m² were excluded from the study.

Ethical approval and patient consent

This study was approval from the ethical committee of Ain Shams University (approval number: FMASU M D 271 / 2019). Before enrollment, written informed consent was obtained from all participants after detailed discussing the purpose for performing the procedure and its duration and potential risks.

Patient data collection

Clinical data, including patient demographics, medical history, and renal function tests (serum creatinine), were recorded for each participant. All patients underwent bilateral digital mammography, CESM, and ultrasound examination. Histopathological findings served as the reference standard for comparison.

Technique

CESM conventional mammography and examinations were conducted using a General Electric Sonograph 2000D full-field mammography system with ultrasonographic (US) complimentary imaging. Patients were asked to fast for six hours before the imaging procedure. Before CESM, patients received a 100 mL intravenous injection of a low-osmolar, non-ionic, monomeric iodinated contrast agent (Ultravist 300. manufacturer: Bayer Corporation, Leverkusen, Germany) at a rate of 3 mL/s through a 20-gauge antecubital vein catheter. Due to its superior safety profile, a low-osmolar iodinated contrast agent was preferred for CESM. If venous access was difficult, a 22-gauge catheter was inserted and the injection rate was adjusted to 2.5 mL/s. Imaging was started 2-8 min after injection to allow the dispersion of the contrast agent within the breast tissue according to the breast density and contrast enhancement. The duration of the imaging procedure was about 10 min.

With the patient was standing, two X-ray images, a low-energy and a high-energy image, were acquired of the same breast location; the low-energy image served as a standard mammogram equivalent, while the high-energy image offered additional details.

Image acquisition and analysis

The low-energy image was digitally subtracted from the high-energy image using the weighted logarithmic technique to enhance the visibility of blood vessels and tumors with a rich blood supply and reduce the appearance of normal breast tissue. Standard images of the examined breast included craniocaudal and mediolateral oblique views. Patients received slightly more radiation than the standard mammogram according to the breast size and composition.

Post-CESM Procedures: Patients were closely monitored during and for at least 30 minutes following the contrast injection, particularly those with no previous exposure to iodinated contrast agents, for any adverse reactions or contrast extravasation. If no side effects of the drug or procedure complications occurred, the intravenous line was removed and patient was discharged. Additionally, breast density was categorized using the American College of Radiology (ACR) classification.

Image Interpretation: Image analysis involved a two-pronged approach: the standard Breast Imaging-Reporting and Data System (BIRADS) scoring system and the specific CESM scoring system. The CESM scoring for high-energy image according to grading of contrast enhancement intensity compared with background enhancement ranged from negative (-1) to intense (2) enhancement. The malignancy potential score (MPS) refers to the sum of the BIRADS and CESM scores and a score <4 indicates a benign lesion, while a score >4 indicates a malignant lesion.

RESULTS

Thirty patients with a history of BCS were included in the study; 27 had ipsilateral (90%) and 3 had bilateral lesions (10%) for a total number of the examined breasts of 33 lesions. Patients' enrolment data are shown in table 1. All patients had surgical excision of the presenting breast mass for histopathological examinations.

Breast US detected 18 solid lesions (54.5%), 5 cystic lesions (15.2%), and two mixed cystic and solid lesions (6.1%), while failed to detect a lesion in 8 cases (24.2%). Regarding lesion' vascularity, US defined 27 non-vascular lesions (81.8%), 4 lesions

(12.1%) showed mild vascularity and two lesions (6.1%) with high vascularity (table 2).

Table 1. Patients' data.

Data		Findings
Вата		
	<40	4 (13.3%)
	40-49	13 (43.4%)
Age (years)	50-59	9 (30%)
	≥60	4 (13.3%)
	Average	49.4±9.2
Latarality of the	Left	17 (56.7%)
Laterality of the lesions	Right	10 (33.3%)
lesions	Bilateral	3 (10%)
	<5	14 (46.7%)
Duration since BCS	5-9	14 (46.7%)
Duration since BCS	≥10	2 (6.6%)
	Average	4.65±2.8

Table 2. US findings.

Item	Findings	Frequency, n; %
Tune of	No lesion	8 (24.2%)
Type of breast	Cystic lesion	5 (15.2%)
lesion	Solid lesion	18 (54.5%)
lesion	Mixed cystic & Solid lesion	2 (6.1%)
Vocavilarity of	Non-vascular	27 (81.8%)
Vascularity of the lesion	Mild vascularity	4 (12.1%)
the lesion	Vascular	2 (6.1%)

Low-energy findings on interpretation of mammographic images were mostly ill-defined lesions in 16 breasts (48.5%) or lesions showing architectural distortions in 9 breasts (27.3%) and defined lesions in 4 breasts (12.1%), while no lesion was detected in the remaining 4 breasts (12.1%). Suspicious calcification was detected in 5 lesions (15.2%) and benign calcification in 6 lesions (18.1%), while no calcification was detected in 22 lesions (66.7%). According to ACR grading for breast density, 17 (51.6%) and 14 breasts (42.4%) were of grades B and C, respectively and one breast (3%) of each of grade A and D. Twenty-four lesions (72.7%) are of BIRADS scoring of <4; 5 (15.2%), 7 (21.2%) and 12 (36.4%) lesions are of BIRADS scores; 1, 2, and 3, respectively. One lesion was scored as both 4 and 4B, two lesions (6.1%) were of score 4A and three lesions (9%) were scored as 4C, and two lesions (6.1%) were of BIRADS score 5 (table 3).

The interpretation of CESM findings defined no enhancement in 20 lesions (60.6%), mild enhancement (30.3%), moderate enhancement in one lesion (3%), and intense enhancement in two lesions (6.1%). According to CESM score, 18 lesions (54.5%) were scored by 0, and 11 lesions (33.3%) were scored by one, while three lesions (9.1%) were scored by 2 and a lesion (3%) by -1.

The calculated MPS defined 19 lesions (67.7%) had a score of <4 which suggests that the lesion is mostly benign, and 14 lesions (42.4%) were scored by \geq 4, a score suggesting that the lesion is most probably to be malignant. Considering pathological diagnosis is the gold standard for comparison, it diagnosed 23 lesions (67.7%) as benign lesions, and 10 lesions (33.3%) as malignant ones (table 4, figure 1).

Table 3. Mammographic findings and scorings.

Low-energy findin	gs	Calcifi	cation		ACR	BIR	ADS Score
Findings	Frequency	Findings	Frequency	Grade	Frequency	score	Frequency
No Lesion	4 (12.1%)	Absent	22 (66.7%)	Α	1 (3%)	1	5 (15.2%)
Architectural Distortion	9 (27.3%)	Benign	6 (18.1%)	В	17 (51.6%)	2	7 (21.2%)
Ill-defined lesion	16 (48.5%)	Suspicious	5 (15.2%)	С	14 (42.4%)	3	12 (36.4%)
Defined lesion	4 (12.1%)			D	1 (2%)	4	1 (3%)
						4A	2 (6.1%)
						4B	1 (3%)
						4C	3 (9%)
						5	2 (6.1%)

Table 4. CESM finding and MPS score, and pathological findings.

	Item	Findings	Frequency, n; %
		No	20 (60.6%)
		Mild	10 (30.3%)
	Enhancement	Moderate	1 (3%)
CESM		Intense	2 (6.1%)
CESIVI		-1	1 (3%)
	Caara	0	18 (54.5%)
	Score	1	11 (33.3%)
		2	3 (9.1%)
	Collectively	<4	19 (57.6%)
	Collectively	≥4	14 (42.4%)
		1	4 (12.1%)
		2	8 (24.2%)
MPS		3	7 (21.2%)
	Differentially	4	9 (27.3%)
		5	2 (6.1%)
		6	2 (6.1%)
		7	1 (3%)
Pathol	ogical diagnosis	Benign	23 (67.7%)
Fatiloi	ogicai diagnosis	Malignant	10 (33.3%)

A comparison of the radiologic findings to the pathological diagnosis, defined high sensitivity and negative predictive values for the MSP score, while the CESM score showed high specificity and positive predictive values. However, the MSP score showed the highest accuracy percentage with the highest 95% confidence interval (table 5).

Table 5. The diagnostic performance values of the radiologic studies.

CESM score 57.14(95% CI:28.86-82.34) 89.47(95% CI:66.86-98.7) 80(95% CI:49.98	MSP score 90(95% CI:55.5 -99.75) 78.26(95% CI: 56.3-92.54 64.29(95% CI:
CI:28.86-82.34) 89.47(95% CI:66.86-98.7)	-99.75) 78.26(95% CI: 56.3-92.54
89.47(95% CI:66.86-98.7)	78.26(95% CI: 56.3-92.54
CI:66.86-98.7)	56.3-92.54
80(95% CI:49.98	64 29(95% CI:
	1 0 1.23(33/0 Cl.
-94.12)	44.65-80.1)
73.91(95%	94.74(95% CI:
CI:60.28-84.1)	73.5-99.15)
75.76(95% CI:	81.82(95% CI:
57 74-88 91)	64.54-93
	CI:60.28-84.1)

95% CI: 95% confidence interval.

Cases demonstration

Case 1: A 32-year-old woman with a history of left breast-conserving surgery presented with a growing lump in the surgical bed. Digital mammography demonstrated focal architectural distortion and an ill-defined soft tissue density at the previous cancer site (BI-RADS 4). Contrast-enhanced

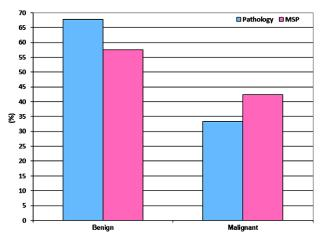


Figure 1. The diagnosis of the studied lesions the MSP.

spectral mammography (CESM) revealed an intensely heterogeneous enhancing lesion corresponding to the clip marker, with associated regional non-mass enhancement and enlarged axillary lymph nodes. The CESM score was 2, and the malignant potential score (MPS) was 6. Histopathology confirmed recurrent invasive ductal carcinoma (Figure 2). A: Craniocaudal mammogram. B: Craniocaudal CESM. C: Mediolateral oblique mammogram. D: Mediolateral oblique CESM.

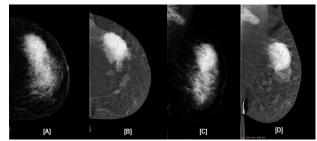


Figure 2. CESM characterization of recurrent invasive ductal carcinoma in a post-lumpectomy patient.

Case 2: a 46-year-old woman with a history of left breast-conserving surgery presented with an enlarging left breast lump. While mammography showed changes consistent with post-surgical effects (diffuse skin thickening and architectural distortion in the upper outer quadrant, BI-RADS 2), CESM revealed a discordant finding: a focal area of faint, heterogeneous non-mass enhancement in the central

lower quadrant. The CESM score was 0, and the malignant potential score (MPS) was 2. Histopathology confirmed mastitis and fat necrosis (Figure 3). A: Craniocaudal mammogram. B: Craniocaudal CESM. C: Mediolateral oblique mammogram. D: Mediolateral oblique CESM.

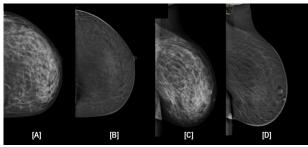


Figure 3. CESM in benign post-lumpectomy changes.

Case 3: A 41-year-old woman with a history of left mastectomy presented with right breast swelling. Mammography showed increased skin thickness, trabeculation, nipple retraction, and a retro-areolar density (BI-RADS 3). CESM demonstrated diffuse enhancement of the thickened skin and breast tissue, predominantly in the retro-areolar region. The CESM score was 2, and the malignant potential score (MPS) was 5. Histopathology confirmed invasive carcinoma with mixed ductal and lobular features (Figure 4). A: Craniocaudal mammogram. B: Craniocaudal CESM. C: Mediolateral oblique mammogram. D: Mediolateral oblique CESM.

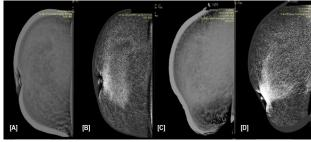


Figure 4. CESM detection of invasive carcinoma in the contralateral breast post-mastectomy.

Case 4: A 41-year-old woman, previously treated for right breast cancer with breast-conserving surgery, presented with diffuse breast edema extending to the contralateral (left) Mammography demonstrated ill-defined lesions and microcalcifications in the left upper outer quadrant, prompting a BI-RADS 4 assessment. Subsequent CESM demonstrated marked contrast uptake consistent with active glandular tissue. The CESM score was 1, and the malignant potential score (MPS) was 5. Histopathology confirmed invasive ductal carcinoma (IDC) and invasive lobular carcinoma (ILC) (Figure 5). A: Craniocaudal mammogram. B: Craniocaudal CESM. C: Mediolateral oblique mammogram. D: Mediolateral oblique CESM.

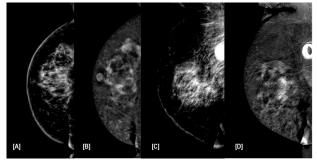


Figure 5. CESM detection of contralateral breast cancer in a patient with post-lumpectomy lymphedema.

DISCUSSION

Histopathological diagnosis of the excised 33 specimens categorized lesions into 23 benign (67.7%) and 10 malignant (33.3%) lesions. Malignant lesions typically exhibited abnormal contrast enhancement within the surgical site, accompanied by irregular shapes, spiculated margins, and heterogeneous enhancement. Benign lesions, conversely, demonstrated no or minimal contrast uptake, with well-defined borders and homogeneous enhancement.

Comparison of CESM and pathology results yielded 8 true positives (24.2%) and 17 true negatives (51.5%). Further the use of the sum of the BI-RADS and the CESM scores to yield the MSP score improved the diagnostic performance of radiologic assessments of breast lesions and raised the frequency of detecting TPs to 9 lesions (27.3%) and TNs to 18 lesions (54.4%). The detected superiority of CESM in characterizing lesion size, extent, and multiplicity compared to conventional mammography (MG) and ultrasound (US).

Numerous earlier studies have demonstrated the superior diagnostic performance of CESM relative to conventional mammography. Diekmann et al. (11) reported improved sensitivity and specificity when MG was combined with CESM. Dromain et al. (12) found CESM to be effective in identifying tumor angiogenesis with higher sensitivity than MG (93% vs. 78%). Thereafter, Fallenberg et al. (14) and Kamal et al. (10) observed a significantly higher detection rate of malignant breast lesion with CESM than MG. and Helal et al. (5) reported sensitivity and specificity of 91.17% and 75% for CESM in detecting recurrent breast cancer with significantly higher detection rates than MG; 50% and 22%, respectively. Also, while et al. (14) found that CESM had a 91.17% sensitivity, a specificity 75.00% and 82.85% accuracy for detection of recurrent breast lesions, and Nada et al. (3) reported greater diagnostic accuracy following CESM administration than FFDM in postoperative breast cancer patients having architectural distortion with increased breast density.

Recently, Hua et al., (15) who investigated the utility of the BI-RADS in CESM in the differentiation of breast non-mass enhancement (NME) lesions and documented that the applied scoring can significantly improve the diagnostic accuracy compared with BI-RADS (MG) and provided specific advantages for NME with micro-calcifications than BI-RADS (MRI). Also, Sanders et al., (16) found screening examinations for mean glandular dose per breast was higher for CESM than for full-field digital mammography or digital breast tomosynthesis alone. Further, Xu et al., (17) detected high diagnostic value of CESM with kinetic enhancement with 100% sensitivity and NPV for BI-RADS 3-5 papillary breast lesions. Moreover, Long et al., (18) documented that the presence of enhancement and morphology on CESM assessment were identified as independent predictors of malignant calcifications of BI-RADS 4B.

In support of the efficacy of CSEM, Ferrara et al., (19) documented moderate agreement and high reproducibility in breast background parenchymal enhancement assessment between MRI and CESM. Furthermore, multiple recent studies demonstrated the implementation of contrast enhancement in protocols for breast assessments using various diagnostic modalities. Hu et al., (20) found that combining contrast-enhanced ultrasonography with CA15-3, HER-2, and sE-cad levels facilitated the differentiation of benign and malignant breast lesions and allowed differentiation between ductal carcinoma in situ and invasive ductal carcinoma, depending on CEUS's ability to show differences in enhancement characteristics and to detect perfusion defects and peripheral high enhancement associated with DCIS (21).

The generalizability and interpretation of this study's findings should be considered in light of several limitations. The retrospective, singleinstitution design and physician-directed use of CESM introduce selection bias, likely favoring patients with dense breasts. The absence of a standardized lexicon for interpreting CESM images, unlike that used for DCE-MRI, has led to subjective interpretation and inconsistent management strategies, including variations in subsequent imaging, follow-up, and biopsy. Additionally, the inclusion of early cases may have contributed to a higher recall rate and more likely benign classifications, potentially reflecting a learning curve effect.

CONCLUSION

CESM outperforms conventional mammography, even when combined with the US, in detecting breast cancer, particularly in patients with breast masses after BCS, and has the potential to significantly improve cancer detection rates compared to routine mammography alone.

Acknowledgments: The authors thank the patients for their participation in our study. Also, the authors thanks the staff members of Be-Check for proofreading and adjusting the article.

Human ethics and consent to participate: Prior to enrollment, written informed consent was obtained from all participants. This study received approval from the ethical committee of Ain Shams University (approval number: FMASU M D 271 / 2019).

Consent for publication: All authors have reviewed the manuscript thoroughly and consent to its publication.

Availability of data and materials:

The datasets used and/or analyzed during the current study are available from the corresponding author upon reasonable request.

Informed Consent: Informed consent was obtained from all the legally authorized representatives of the participants included in the study.

Conflict of Interest Statement: The authors declare no competing interests.

Funding declaration: Authors confirmed that no fund received from any organization and the research done by their own.

Authors' contributions: DAMS led the research idea, study design, and wrote the initial draft. AAB handled data curation, analysis, and manuscript review. NAETC conducted experiments, collected data, and supervised the research. MAMN managed visualization, project administration, and funding acquisition.

REFERENCES

- Lee CH, Phillips J, Sung JS, et al. (2024) Contrast enhanced mammography (CEM) (A supplement to ACR BI-RADS® mammography). American College of Radiology.
- Azim HA and Ibrahim AS (2014) Breast cancer in Egypt, China and Chinese: statistics and beyond. *Journal of Thoracic Dis*, 6(7): 864-866. doi: 10.3978/j.issn.2072-1439.2014.06.38.
- Nada O, El Fiky S, Chalabi N, et al. (2021) Role of contrast enhanced spectral mammography after conserving brest surgery. Ain Shams Medical Journal, 72(4): 767-779. doi: 10.21608/asmj.2021.222682.
- Siegel RL, Miller KD, Jemal A (2019) Cancer statistics, 2019. CA: A Cancer Journal for Clinicians, 69(1): 7-34. doi: 10.3322/caac.21551.
- Helal M, Abu Samra M, Ibraheem M, et al. (2017) Accuracy of CESM versus conventional mammography and ultrasound in evaluation of BI-RADS 3 and 4 breast lesions with pathological correlation. The Egyptian Journal of Radiology and Nuclear Medicine, 48: 741-750. doi: 10.1016/j.ejrnm.2017.03.004.
- Petit JY, Veronesi U, Luini A, et al. (2005) When mastectomy becomes inevitable: the nipple-sparing approach. Breast, 14(6): 527-531. doi: 10.1016/j.breast.2005.08.028.
- Zeeneldin AA, Ramadan M, Gaber AA, et al. (2013) Clinicopathological features of breast carcinoma in elderly Egyptian patients: a comparison with the non-elderly using populationbased data. *Journal of the Egyptian National Cancer Institute*, 25 (1): 5-11. doi: 10.1016/j.jnci.2012.10.003.
- Yousef AF, Khater HM, Jameel LM (2018) Contrast-enhanced spectral mammography versus magnetic resonance imaging in the assessment of breast masses. Benha Medical Journal, 35: 5-12.
- Patel BK, Lobbes MBI, Lewin J (2018) Contrast Enhanced Spectral Mammography: A Review. Semin Ultrasound CT MR, 39(1): 70-79. doi: 10.1053/j.sult.2017.08.005.
- 10. Kamal RM, Helal MH, Wessam R, et al. (2015) Contrast-enhanced spectral mammography: Impact of the qualitative morphology descriptors on the diagnosis of breast lesions. European Journal of

- Radiology, **84**(6): 1049-1055. doi: 10.1016/j.ejrad.2015.03.005.
- 11. Diekmann F and Bick U (2007) Tomosynthesis and contrastenhanced digital mammography: recent advances in digital mammography. *European Radiology*, *17*(12): 3086-3092. doi: 10.1007/s00330-007-0715-x.
- Dromain C, Thibault F, Diekmann F, et al. (2013) Dual-energy contrast-enhanced digital mammography: initial clinical results of a multireader, multicase study. Breast Cancer Research, 14(3): R94. doi: 10.1186/bcr3210.
- 13. Fallenberg EM, Dromain C, Diekmann F, et al. (2014) Contrastenhanced spectral mammography versus MRI: Initial results in the detection of breast cancer and assessment of tumour size. Eur Radiol, 24(1): 256-264. doi: 10.1007/s00330-013-3007-7.
- 14. While A, Krupinski E, Mordang JJ, et al. (2019) Detection of breast cancer with mammography: effect of an artificial intelligence support system. Radiology, 290(2): 305-314.
- Hua B, Chen J, Li QR, et al. (2025) Breast non-mass enhancement lesions on contrast-enhanced mammography: modified breast image reporting and data system classification. Clin Radiol, 83: 106807. doi: 10.1016/j.crad.2025.106807.
- 16. Sanders JW, Pavlicek W, Stefan W, et al. (2025) Digital mammography, tomosynthesis, and contrast-enhanced mammography: intraindividual comparison of mean glandular dose for screening examinations. Am J Roentgenol, 224(3): e2432150. doi: 10.2214/AJR.24.32150.

- 17. Xu W, Chen L, Zeng W, et al. (2025) Addition of contrast-enhanced mammography enhancement patterns and morphology for differentiating benign from malignant papillary breast lesions. Br J Radiol, 98(1167): 383-391. doi: 10.1093/bjr/tqae241.
- 18. Long R, Luo Y, Cao M, et al. (2025) Malignancy risk stratification prediction of BI-RADS 4B calcifications based on contrast-enhanced mammographic features: a multicenter study. Breast Cancer Res Treat, 210(1): 135-145. doi: 10.1007/s10549-024-07546-w.
- Ferrara F, Santonocito A, Vogel W, et al. (2025) Background parenchymal enhancement in CEM and MRI: Is there always a high agreement? Eur J Radiol, 183: 111903. doi: 10.1016/ j.ejrad.2024.111903.
- 20. Hu K, Wang Y, Ma Y, et al. Clinical utility of quantitative ultrasonography parameters combined with serum cancer antigen 15-3, human epidermal growth factor receptor 2 and soluble E-cadherin in diagnosing mass®type breast cancer. Oncol Lett, 29(3): 133. doi: 10.3892/ol.2025.14879.
- 21. Li W, Zhao Y, Fei X, et al. (2025) Image features and diagnostic value of contrast-enhanced ultrasound for ductal carcinoma in situ of the breast: Preliminary findings. *Ultrason Imaging*, **47**(2): 59-67. doi: 10.1177/01617346241292032.